Talanta 287 (2025) 127588

Contents lists available at ScienceDirect

Talanta

journal homepage: www.elsevier.com/locate/talanta

In situ biosensing for cell viability and drug evaluation in 3D extracellular matrix cultures: Applications in cytoprotection of oxidative stress injury

Yu Zhong, Meng-Meng Liu, Xia Cao, Yun Lei **, Ai-Lin Liu *

Department of Pharmaceutical Analysis, Higher Educational Key Laboratory for Nano Biomedical Technology of Fujian Province, Faculty of Pharmacy, Fujian Medical University, Fuzhou, 350122, China

ARTICLE INFO

Keywords:
Oxidative stress injury
3D agarose hydrogel
Electrochemical biosensing assay
Un/low/highly/NGF-Differentiated PC12 cell lines
Catecholamine neurotransmitter
Exosome

ABSTRACT

The rise of extracellular matrix (ECM)-supported three-dimensional (3D) cell culture systems which bridge the gap between *in vitro* culture and *in vivo* living tissue for pharmacological models has increased the need for simple and robust cell viability assays. This study presents the development of an effective biosensing assay for *in situ* monitoring of the catecholamine neurotransmitter exocytosis levels for cell viability assessment within complicated cell-encapsulated hydrogel milieu. Firstly, the biosensing assay demonstrated the distinction among four pheochromocytoma (PC12) cell lines with varying degrees of differentiation and the discrepancy in cellular neurosecretory capacity between two-dimensional (2D) monolayer and 3D agarose hydrogel culture conditions, accompanied by morphological distinctions. Secondly, the electrochemical biosensing assay was performed for viability monitoring of PC12 cell lines following various treatments, including oxidative stress injury (OSI) induced by H_2O_2 and intervention protected by nimodipine, bone marrow mesenchymal stem cells (BMMSC) supernatant and BMMSC-derived exosomes under 2D and 3D milieus. Of note, BMMSC-derived exosomes exhibited high cytoprotection, anti-oxidation effect, endogenous esterase activity and membrane integrity against OSI. Collectively, the biosensing assay results showed principal but not entire consistency with that of conventional cell-counting kit-8 assay. Therefore, the developed biosensing assay allows for sensitive and *in situ* cell viability assays in spatial ECM environment, which has broad applications in monitoring physiological and pathological processes.

1. Introduction

Owing to its high metabolic rate and relatively poor cellular regeneration capacity, the brain is particularly susceptible to oxidative stress injury (OSI) [1]. Oxidative stress reflects the disruption of an intricate balance between the production of oxidants and the antioxidant defense mechanism, and is implicated in neurodegenerative diseases (ND) caused by various genetic or environmental insults, such as Parkinson's disease (PD), Alzheimer's disease (AD), epilepsy, amyotrophic lateral sclerosis (ALS), Huntington's disease (HD), *etc.* [2,3]. As such, the application of cell culture-based methodology in OSI studies is of great importance to discern the role and pathogenesis of oxidative stress in ND. Conventional flask-based two-dimensional (2D) cell culture partly compromises the clinical relevance and hampers predictive capacity due to the lack of cell-cell and cell-extracellular matrix (ECM) interactions [4]. In this regard, three-dimensional (3D) cell culture increases the dimensionality of ECM around the cells and recovers cellular spatial organization [5]. Specifically, 3D cell culture answers to retaining natural cell shape, allows gradient availability of media components, and permits high cell viability and proliferation [6]. Currently, hydrogels as 3D scaffolds for hosting cells possess swelling feature (ability to swell but without dissolving in water), 3D viscoelastic networks, good biocompatibility and high permeability for nutrients and oxygen, which greatly imitate the built-in bioactivity of ECM architecture [7,8]. For instance, Zhang et al. reported that MIN6 cells cultured in 3D tunable hydrogel exhibited greatly increased insulin synthesis and glucose sensitivity compared to planar culture [9].

To alleviate oxidative stress damage, a variety of synthetic or natural antioxidants, drugs and bioactive substances have been assessed in preclinical studies concerning ND [10–12]. Among them, bone marrow mesenchymal stem cells (BMMSC), a type of fibroblast-like pluripotent adult stem cells, have attracted great attention due to their autologous

* Corresponding author.
** Corresponding author.
E-mail addresses: leiyun@fjmu.edu.cn (Y. Lei), ailinliu@fjmu.edu.cn (A.-L. Liu).

https://doi.org/10.1016/j.talanta.2025.127588
Received 8 July 2024; Received in revised form 30 October 2024; Accepted 11 January 2025
Available online 13 January 2025
0039-9140/© 2025 Elsevier B.V. All rights are reserved, including those for text and data mining, AI training, and similar technologies.

source, wide availability and low tumorigenicity [13]. BMMSC-based therapeutic approaches mainly involve cellular replacement therapy and paracrine effect [14]. The latter indirectly influences the neurocellular niche via release of neuroprotective factors and constituents to induce or enhance neurogenesis [15]. Of note, via paracrine-mediated mechanism, exosomes (membrane-enclosed vesicles with a size of 30–150 nm, containing proteins, lipids, and microRNAs from their parent cells) can shuttle through intracellular vesicles to exert therapeutic effects against OSI [16]. Additionally, BMMSC-derived exosomes possessed merits of stability in circulation and low immunogenicity [17], exhibiting promising potential as a biotherapy to boost the recipient cell function.

For the evaluation of therapeutic strategies to ameliorate OSI, the measurement of cell viability is the principal response for evaluating the effect of experimental treatments, especially in preclinical studies. Till now, cell-based assays for evaluating viability have predominantly been measured with microplate readers, flow cytometers, or high content imaging [18,19]. Among them, the most commonly used method in laboratories is colorimetric assay, such as 3-(4,5-dimethyl-2-thiazolyl)-2,5-diphenyl-2*H*-tetrazolium bromide (MTT) and cell counting kit-8 (CCK-8), due to their high sensitivity, standardized readout and simple operation [20,21]. However, MTT and CCK-8 results may be assay-dependent, as evidenced by Jiao et al.'s inconsistent cell viability results for both assays in the cytotoxicity test of graphene [22]. Our previous findings underscored notable functional differences between mitochondrial enzyme activity and neurosecretory activity in 2D cell culture [23]. Worse still, spectroscopic interference may occur when colored exogenous substances are introduced. Notably, due to the technical complexity of multilayer-3D cell viability assay, colorimetric results may lead to false-positive or false-negative results [24], and optical measurements often require the expensive confocal microscopy or even two-photon microscopy. Furthermore, colorimetric assays are end-point and non-real-time owing to a certain incubation time requirement. Consequently, a sensitive, real-time and *in situ* viability assay is an urgent need in 3D cell culture system. Electrochemical biosensing method holds great promising potential for assessment of cell viability via directly converting biologically functional signals (secretory or expression capacity of specific substances, such as neurotransmitters, reactive oxygen species, reactive nitrogen species, adenosine triphosphate, enzyme activity, *etc.*) into electrical signals [25–27]. Electrochemical analysis unfolds considerable merits of low detection limit, rapid response, portability, high selectivity, cost-effectiveness and minimal expertise requirements [28,29], further indicating its advantages in viability assay. On-line electrochemical monitoring of exocytosis of catecholamine neurotransmitters from living cells cultured in 3D milieu can reflect the pathophysiological state in real time, surmounting the technical barriers of 3D cell viability through colorimetric and imaging assays and serving as promising candidates for drug screening and toxicity assessment.

In this work, to surmount the limitations inherent to 2D models, we integrated 3D cell culture techniques to advance to a more physiologically relevant assessment of cellular functions, thereby comparatively analyzing neurosecretion and mitochondrial enzymatic activities within a 3D framework. In response to the challenge of 3D cell viability assay, we developed an electrochemical biosensing assay to *in situ* assess oxidative stress-dependent cell damage and drug efficacy through monitoring the neurosecretory capacity in 3D agarose hydrogel milieu. As shown in Scheme 1, the prepared electrochemical biosensor (screen-printed carbon electrode modified with gold nanostructures and Nafion, abbreviated as Nafion/AuNS/SPCE) was used to distinguish the exocytosis capacity of catecholamine neurotransmitters (represented by dopamine, DA) of four pheochromocytoma (PC12) cell lines with various treatments. Of note, PC12 cell lines possess merits of homogeneous and unlimited propagation, capacity to undergo neuronal differentiation, and exocytosis of catecholamines and acetylcholine, which have been widely used for establishing OSI cell models [23,30–32]. Different PC12 cell lines were used to mimic neurons with different degrees of differentiation for investigating the levels of neurotransmitter release and evaluating drug intervention under OSI condition. For intervention evaluation, the neuroprotective effect of nimodipine, BMMSC supernate and BMMSC-derived exosomes was investigated. On the comparison of 2D flat culture and 3D agarose hydrogel-encapsulated culture, proliferation rate and neurosecretory capacity were studied. The electrochemical biosensing of cell viability following different treatments, accompanied by the traditional colorimetric assay, demonstrated an improvement in cellular stimuli-sensitivity to a degree under the 3D cell culture system. The viability results obtained by those two assays were basically but not entirely consistent, which may be due to the different assessing factors. Collectively, the developed electrochemical biosensing assay can realize *in situ*, real-time, accurate and sensitive evaluation of real cellular pathophysiological conditions. As an auxiliary method for assessing cell viability, electrochemical biosensing assay is expected to be used in various cellular processes of PC12 cells, such as cell differentiation, intervention, senescence, apoptosis, *etc*.

2. Experimental section

Reagents, apparatus, construction and characterization of Nafion/AuNS/SPCE, construction and intervention of OSI models, isolation and characterization of BMMSC-derived exosomes, cytotoxicity of

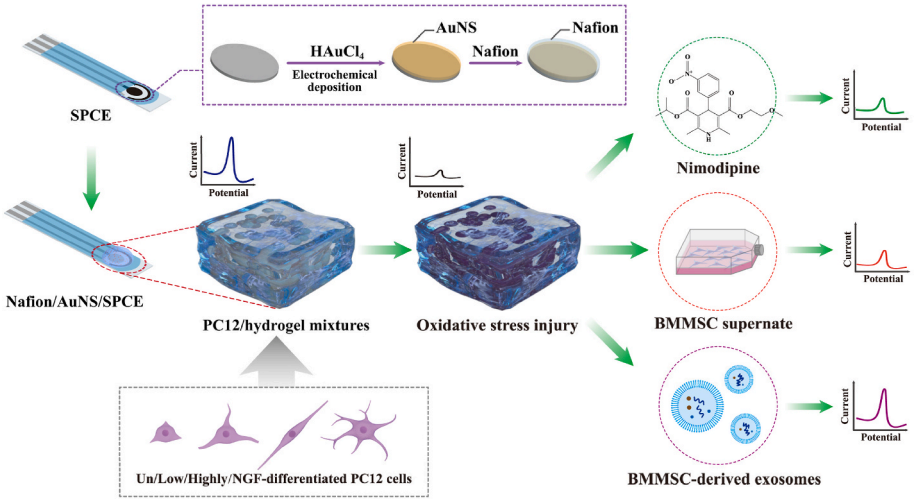

Scheme 1. Schematic illustration of *in situ* cell viability and drug evaluation biosensing assay for catecholamine neurotransmitters released from living PC12 cells.

nimodipine can be referred in Supplementary Information.

3. Results and discussion

3.1. Characterization of cell morphology

The PC12 cell lines, firstly cloned by Greene and Tischle from a pheochromocytoma tumor, possess merits of homogeneous propagation in the unlimited way, capacity to undergo neuronal differentiation in response to nerve growth factor (NGF), and neuroendocrine secretion (catecholamines and acetylcholine), which are greatly used in neurological disease modeling [23,30–32]. To evaluate the versatility of the developed biosensing assay, we adopted and monitored multiple PC12 cells, consisting of the purchased PC12 cells with various degrees of differentiation (un/low/highly-differentiated PC12 cells) and the self-made NGF-induced low-differentiated PC12 cells (NGF-differentiated PC12 cells).

The morphology and proliferation ability of un/low/highly/NGF-differentiated PC12 cells were observed by scanning electron microscope (SEM) and confocal laser scanning microscope (CLSM). As shown in Fig. 1A, under 2D culture, undifferentiated PC12 cells grew as uniformly spherical shaped, floating cell clusters or as a few scattered lightly attached cells. Low-differentiated PC12 cells were polygonal and round in a few (Fig. 1B). The morphology of highly-differentiated PC12 cells was fusiform (Fig. 1C). In Fig. 1D, NGF-differentiated PC12 cells (low-differentiated PC12 cells after exposure to 50 ng/mL NGF for 7 days) displayed a substantial increase in neurite length. The CLSM images showed four PC12 cell lines in medium (Fig. 1E–H) and hydrogel-encapsulated ambience (Fig. 1I–L). The proliferative ability of four PC12 cell lines was reflected by fluorescent intensity with respect to living PC12 cells (initial number: 1×10^4) stained with 0.1% calcein acetoxymethyl ester after 48 h of culture. The highly-differentiated PC12 cells possessed greatest growth rate (Fig. 1G), while the undifferentiated PC12 cells had the lowest counterpart among the four cell lines (Fig. 1E). The NGF-differentiated PC12 cells recovered their proliferative ability after replaced with a serum-containing medium (Fig. 1H), resembling their pre-differentiated state (Fig. 1F). This trend was also observed under hierarchically culturing conditions (Fig. 1I–L), indicating a highly biocompatible environment furnished by agarose hydrogels.

3.2. Characterization and analytical performance of Nafion/AuNS/SPCE

The morphology of Nafion/AuNS/SPCE was characterized by SEM. After electrodeposition, AuNS were observed to form clusters in a flower-like hierarchical structure (Fig. 2A), providing a large effective surface for the loading of targeted analytes. Cyclic voltammetry (CV) and electrochemical impedance spectroscopy (EIS) were carried out to reflect the stepwise modification of the electrochemical biosensor. Clearly, in Fig. S1B, the redox peaks of AuNS/SPCE (curve b) were enhanced in a solution containing 1 mM $[Fe(CN)_6]^{3-/4-}$ and 0.1 M KCl as the supporting electrolyte, compared with bare SPCE (curve a). Upon Nafion modification (curve c), the peak current slightly reduced owing to electrostatic repulsion between the negatively charged Nafion and $[Fe(CN)_6]^{3-/4-}$ in solution. The results were further verified in Fig. S1A. Additionally, in Fig. S1C, the charge-transfer resistance (R_{ct}) of the bare SPCE (curve a, 5660 Ω) remarkably decreased with the deposition of AuNS (curve b, 1517 Ω) and Nafion/AuNS (curve c, 1837 Ω).

The analytical performance of the proposed electrochemical biosensor was respectively evaluated in 10 mM PBS (pH 7.4) and 3D decellularized matrix hydrogel. The decellularized matrix hydrogel was obtained by digesting cells with trypsin for 3 h to kill cells, removing trypsin and cleaning cell debris with PBS. Differential pulse voltammetry (DPV) measurements showed the oxidation peak current response

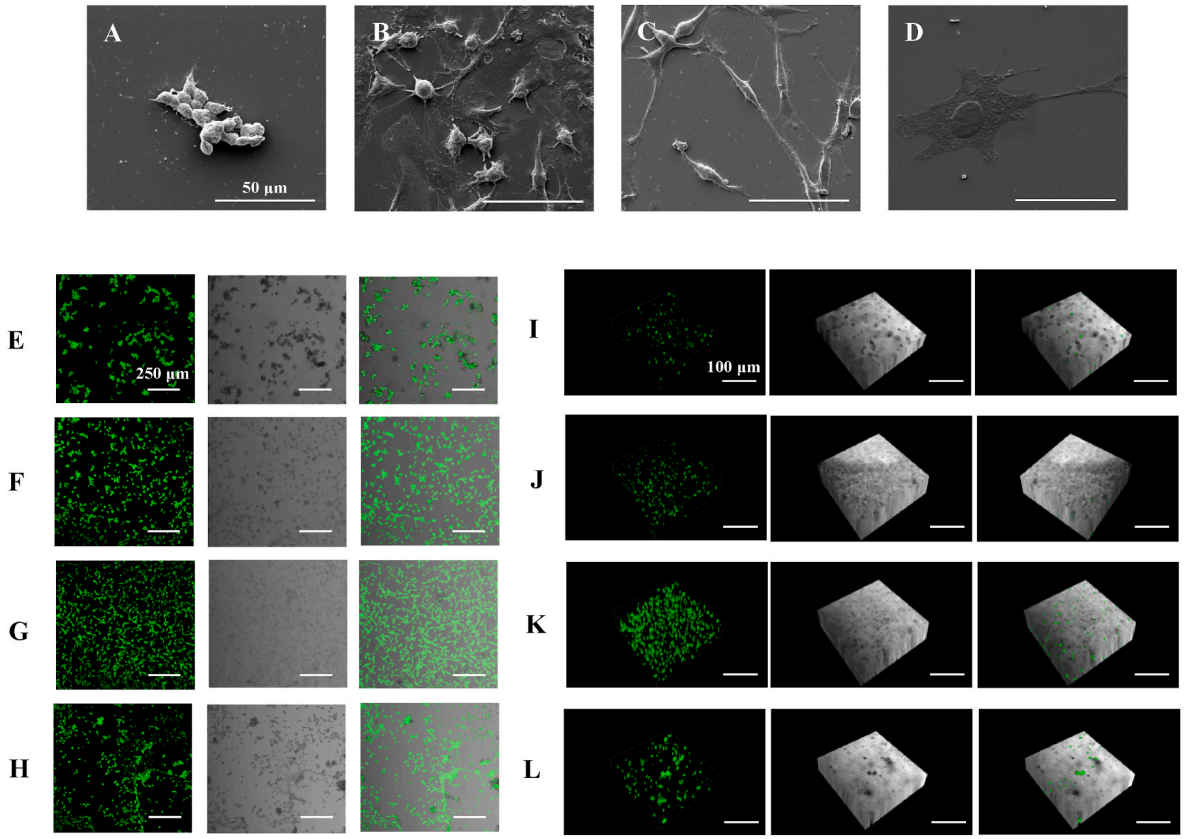

Fig. 1. (A–D) SEM images of un/low/highly/NGF-differentiated PC12 cells under 2D conditions. (E–H) CLSM images of un/low/highly/NGF-differentiated PC12 cells on 2D confocal dishes. (I–L) CLSM reconstruction images of un/low/highly/NGF- differentiated PC12 cells in 3D agarose hydrogels.

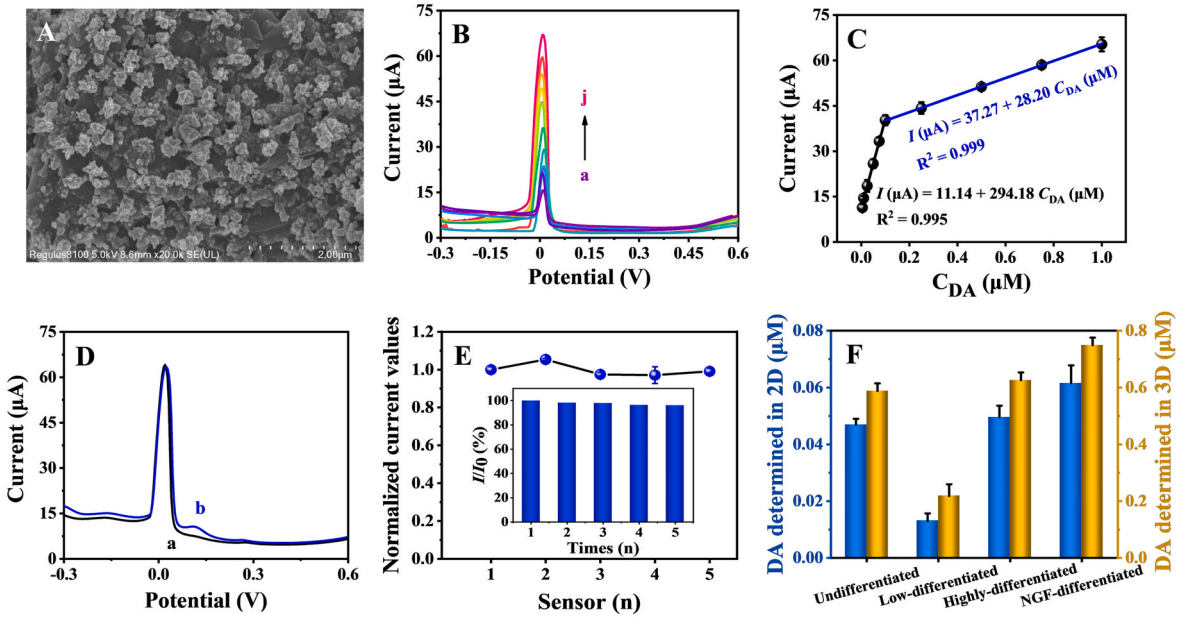

Fig. 2. (A) SEM image of Nafion/AuNS/SPCE. (B) DPV measurements of various concentrations of DA in decellularized matrix hydrogel. (C) Linear relationship between current response values and concentrations of DA. Curves a to j: 0.005, 0.01, 0.025, 0.05, 0.075, 0.1, 0.25, 0.5, 0.75, 1 μM DA (n = 3). (D) DPV responses of 0.5 μM DA (curve a) and 0.5 μM DA in the presence of 50 μM AA, 50 μM UA and 105 mM K^+ (curve b) at Nafion/AuNS/SPCE in decellularized matrix hydrogel. (E) Normalized current values of five distinctive Nafion/AuNS/SPCE to detect 0.1 μM DA in decellularized matrix hydrogel. Insets: the normalized current values at the same biosensor repeated for five times. I_0 was the current value of the first test, I was the current value of the subsequent test. (F) Catecholamine neurotransmitters determination of un/low/highly/NGF-differentiated PC12 cells (about 1.5 × 10^4 cells) under 2D and 3D culture conditions. The data were mean ± standard deviation values of three independent experiments (n = 3). Compared between two groups, ****$P < 0.0001$, ***$P < 0.001$, **$P < 0.01$, *$P < 0.05$, ns > 0.05.

was aggrandized with increasing concentrations of DA (Fig. 2B and Fig. S2). In PBS, the developed biosensor exhibited linearity with DA concentrations from 0.1 nM to 10 nM and 10 nM to 0.1 μM, and the linear regression equations were calculated as I (μA) = 8.29 + 3414.73 C_{DA} (μM) and I (μA) = 40.03 + 255.84 C_{DA} (μM) with the correlation coefficients of 0.999 and 0.992, severally. The limit of detection (LOD, S/N = 3) was 79.8 pM (Fig. S2B). In decellularized matrix hydrogel, the DPV current was linear with DA concentrations ranging from 5 nM to 100 nM and 100 nM to 1 μM. The linear regression equations were I (μA) = 11.14 + 294.18 C_{DA} (μM), R^2 = 0.995, and I (μA) = 37.27 + 28.20 C_{DA} (μM), R^2 = 0.999, with a LOD of 214.9 pM (S/N = 3) (Fig. 2C). There were two separate linear relationships in both PBS and decellularized matrix hydrogel for the following reasons. At low DA concentrations, due to the enhanced diffusive effects on the surface of electrode, even small changes in concentration can contribute to significant change in current response, further resulting in high sensitivity. At high DA levels, the high possibility of fouling the electrode surface by the reaction products may lead to a lower slope. The two separate linear relationships were basically consistent with the literature [33].

In addition, the selectivity of Nafion/AuNS/SPCE toward DA was assessed in the presence of potential co-existing substances in PBS (pH 7.4) (Fig. S3) and decellularized matrix hydrogel (Fig. 2D). The DPV responses showed two distinct peaks at around 0.008 V and 0.15 V were observed, corresponding to the oxidation of DA and uric acid (UA), severally. Ascorbic acid (AA) and K^+ barely affected the current signal. The discrepancy in peak potential and the relatively low peak current of UA demonstrated that the developed biosensor exhibited good selectivity toward DA. To evaluate the intra-group and inter-group reproducibility of Nafion/AuNS/SPCE, the five repetitive measurements on the same biosensor and one measurement on five different biosensors were carried out by DPV measurements of 0.1 μM DA in PBS (pH 7.4) and decellularized matrix hydrogel, respectively. The relative standard deviations (RSD) for successive determinations in PBS and decellularized matrix hydrogel were 0.78% and 1.6%, separately (insets of Fig. S4 and Fig. 2E). The current responses of the biosensor decreased to 98.0% and 96.1% of their original values. Furthermore, as shown in Fig. S4, the RSD of five diverse electrodes under conventional PBS circumstance was 4.36%, while in decellularized matrix hydrogel it was 3.32% (Fig. 2E). These detailed investigations demonstrate the excellent reproducibility of the biosensor. Collectively, these results illustrate the successful construction of the biosensing assay and its feasibility toward DA determination in biological niches with satisfactory accuracy.

3.3. *Electrochemical biosensing assay of DA released from living PC12 cells*

The neurobiological studies concerning monitoring neurotransmitter exocytosis from PC12 cells were performed using the proposed biosensor. Extracellular K^+ could cause depolarization of cell membrane, inducing an influx of Ca^{2+} through opening of voltage-sensitive Ca^{2+} channels and thus evoking the cellular exocytosis of catecholamines and acetylcholine [34]. Analysis of DA secreted by *ca.* 1.5 × 10^4 PC12 cells (Fig. 2F) exhibited that NGF-differentiated PC12 cells secreted the most amount of DA, followed by highly-differentiated and undifferentiated cells, and low-differentiated cells released the least. This gradient indicates the diverse biological capacity among the cell states, corroborating our prior findings [23]. Moreover, 3D-cultured cells had greater secretory capacity than conventional culture, which was attributed to factors such as real-time and *in situ* determination, an increase in specific surface area of cell/hydrogel-stimuli, a relatively slow release rate of K^+, and the enriched DA on electrode surface by mobile colloid property of agarose hydrogel. Furthermore, recovery studies were performed by standard addition methods in both PBS and agarose hydrogel. The recoveries severally lied in the range of 91.2%–123% (Table S1) and 98.4%–114% (Table S2), which could indirectly illustrate the developed biosensor's accuracy for detecting DA in 2D and 3D conditions.

3.4. Construction and intervention of OSI models

As a central player in neurodegenerative diseases, oxidative stress is a pathophysiological response where the disequilibrium between the production of oxidants and the antioxidant defense mechanism occurs and net reactive oxygen/nitrogen species increases [35]. H_2O_2 is widely used to imitate OSI within a short time period [36]. Nimodipine, a dihydropyridine calcium channel blocker, exhibits high affinity and specificity for brain calcium-channel receptors, conferring great neuroprotective effects [37,38]. In this regard, we monitored the H_2O_2 modeling effect and drug intervention effect on four PC12 cell lines under both 2D and 3D conditions, using the CCK-8 assay to gauge cellular mitochondrial dehydrogenase viability as an indicator of cell viability, and the electrochemical biosensing assay to access neurotransmitters secretion capacity, indicative of cell biological activity.

3.4.1. H_2O_2 modeling effect investigation

The cell viability of un/low/highly/NGF-differentiated PC12 cells exposed to H_2O_2 in 2D serum-free medium and 3D agarose hydrogel environments was shown in Fig. 3A–D. As expected, incubation with H_2O_2 caused a significant dose-dependent decrease in cell viability, with the half maximal inhibitory concentrations (IC_{50}) of H_2O_2 displayed in Table S3, which was basically consistent with the studies [39,40]. The four PC12 cell lines exhibited discrepancy in tolerance. Notably, in 2D condition, the IC_{50} values of H_2O_2 determined by electrochemical biosensing assay diverged from those determined by the CCK-8 assay, potentially due to different assessing factors, a finding consistent with our previous study [23]. However, in 3D condition, this difference was significantly reduced, due to the homogeneous culture and stability of cellular function, indicating the superiority of 3D culture. Additionally, the IC_{50} in 3D environment was lower than in 2D environment, attributed to increased cell/hydrogel-H_2O_2 interaction surface area, a slower H_2O_2 release rate, and greater exposure to exogenous injury.

3.4.2. Nimodipine safety and intervention effect study

Firstly, safety evaluation of nimodipine on un/low/highly/NGF-differentiated PC12 cell viability was assessed by CCK-8 assay. As shown in Fig. S5, high concentrations of nimodipine demonstrated high cytotoxicity, thus the range of intervention concentration was chosen at 5–40 μM for 2D and 5–50 μM for 3D conditions. And the relatively slow release rate of nimodipine in the 3D agarose hydrogel mitigated acute toxicity. Then, the optimal intervention concentrations of drug were determined via CCK-8 and electrochemical biosensing assays. Fig. 4A–D depicted a dose-dependent inhibition of cell viability in 2D cultures, with inconsistent results in 3D agarose hydrogel, indicating different drug sensitivities under various culture systems. The electrochemical biosensing assay, aligning with CCK-8 in 3D condition, confirms neurosecretory capacity as a reliable indicator of cell viability and the assay's validity for screening drug efficacy. To compare the intervention effect between 2D and 3D environments, we chose 5 μM nimodipine as intervention concentration, providing a standardized threshold to evaluate the differential impacts of the drug in both culture systems.

3.5. Intervention effect investigation of various substances

BMMSC, as fibroblast-like pluripotent adult stem cells, possesses cytoprotection, anti-apoptosis, immunoregulation and anti-inflammatory functions through paracrine mechanisms [41,42]. Recently, BMMSC intervention methods mainly include BMMSC co-culture, BMMSC supernate and BMMSC-derived substance

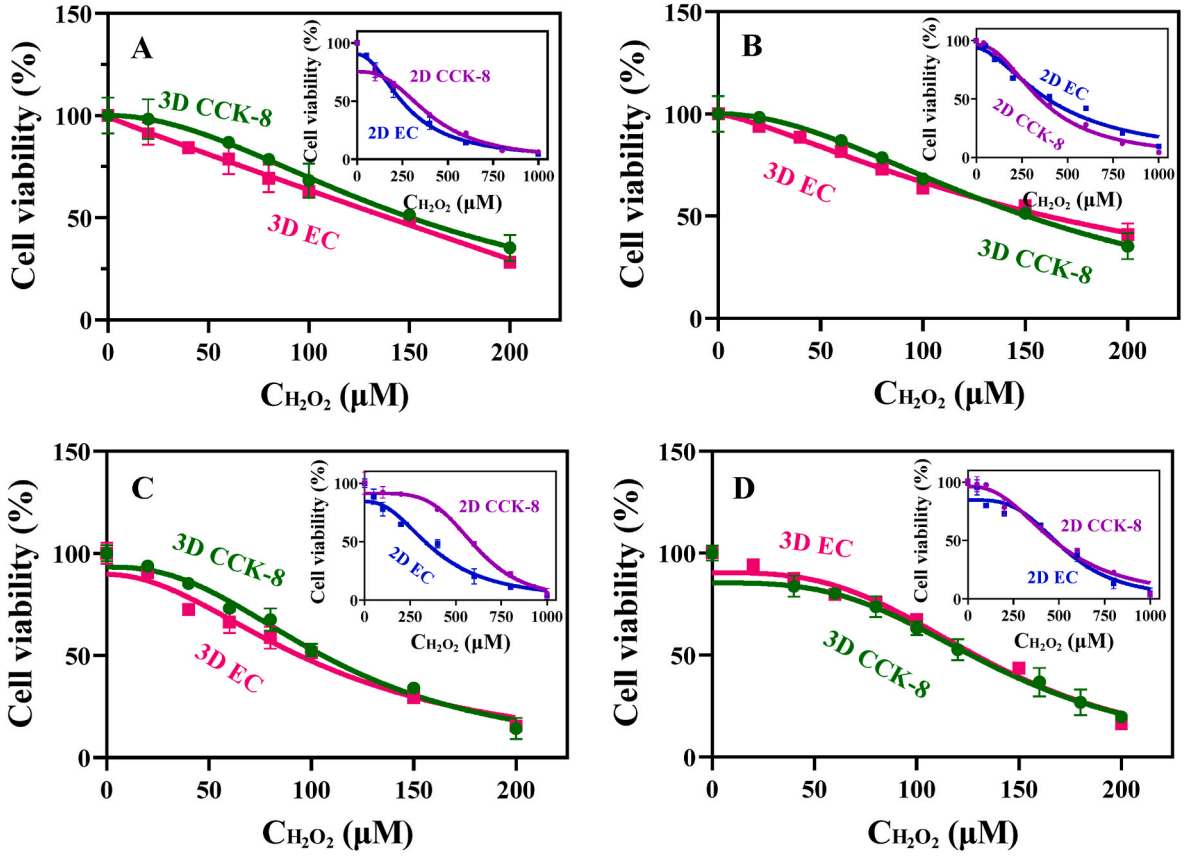

Fig. 3. Effects of H_2O_2 on cell viability of un/low/highly/NGF-differentiated PC12 cells (A–D) under 3D conditions measured by CCK-8 and electrochemical biosensing (abbreviated as EC) assays. Insets: cell viability of four PC12 cells under 2D conditions as above. The data were mean ± standard deviation values of three independent experiments (n = 3).

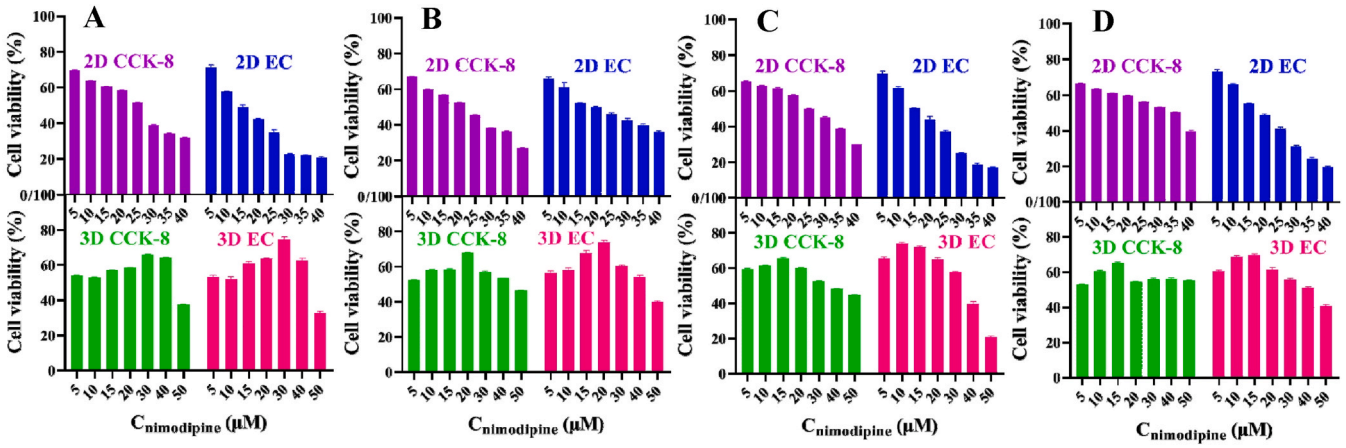

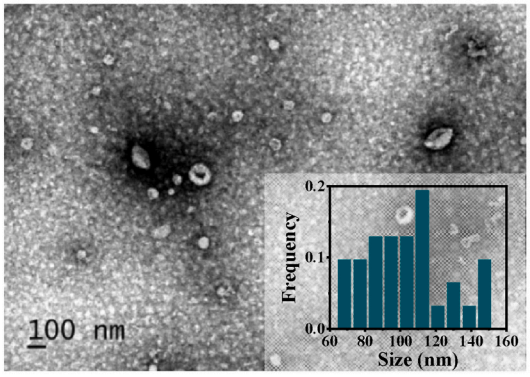

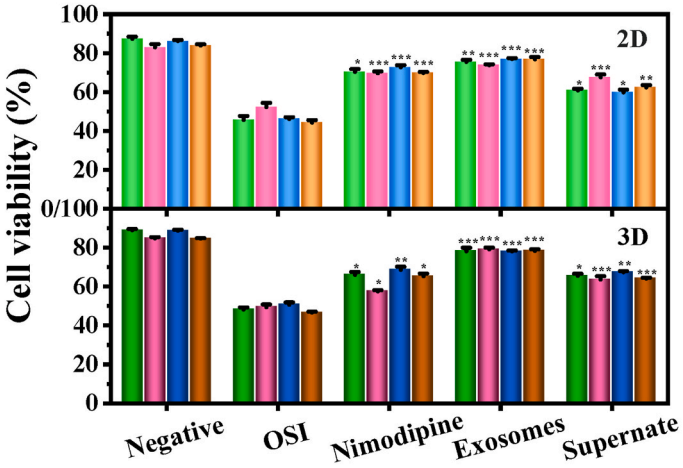

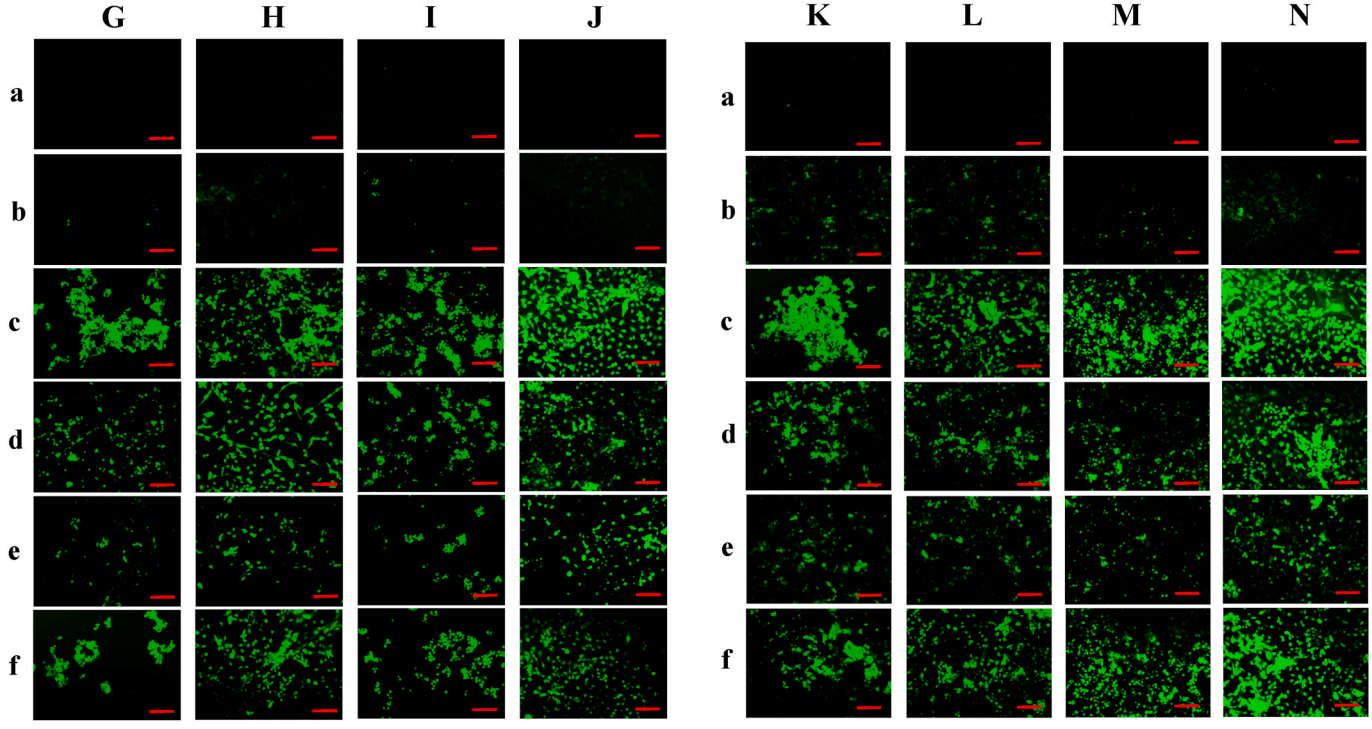

(caption on next page)

Fig. 4. Intervention effects of nimodipine on cell viability of un/low/highly/NGF-differentiated PC12 cells (A–D) measured by CCK-8 and electrochemical biosensing (EC) assays. (E) TEM image of BMMSC-derived exosomes. Inset: size distribution of BMMSC-derived exosomes. (F) Histograms of cell viability corresponding to undifferentiated (green), low-differentiated (pink), highly-differentiated (blue) and NGF-differentiated (brown) PC12 cells determined by electrochemical biosensing assay under 2D (upper) and 3D (lower) milieus in various conditions: culturing with serum-containing RPMI 1640 medium (blank control group, serves as 100%, data not shown), serum-free RPMI 1640 medium (negative control group), exposure to H_2O_2 for 24 h (OSI group), exposure to H_2O_2 for 24 h after pre-treatment with 5 μM nimodipine for 24 h (nimodipine group), exposure to H_2O_2 for 24 h after pre-treatment with 45 μg BMMSC-derived exosomes (exosomes group), and exposure to H_2O_2 for 24 h after pre-treatment with BMMSC supernate for 24 h (supernate group). Compared with OSI modeling group, $^{***}P < 0.001$, $^{**}P < 0.01$, $^{*}P < 0.05$, ns > 0.05. ROS expression of un/low/highly/NGF-differentiated PC12 cells after implementation of intervening with nimodipine, exosomes and BMMSC supernate in 2D (G–J) and 3D (K–N) culture systems. a: blank control group; b: negative control group; c: OSI group; d: nimodipine group; e: exosomes group; f: supernate group (scale bar is 100 μm). (For interpretation of the references to color in this figure legend, the reader is referred to the Web version of this article.)

intervention. Thereinto, BMMSC-derived exosomes (membrane-enclosed vesicles) are capable of regulating recipient cell function through delivering proteins, lipids, RNAs, and other molecular constituents [43]. Importantly, this cargo plays a vital role in stem cell therapy due to their stability in circulation and low immunogenicity [17].

3.5.1. *Characterization and quantification of BMMSC-derived exosomes*

BMMSC-derived exosomes isolated from BMMSC supernate had a typical bilayer structure with a diameter ranging from 40 to 100 nm, as shown in Fig. 4E. Furthermore, the present of tumor susceptibility gene 101 (TSG 101), a protein marker of exosomes, was confirmed by Western blot analysis (Fig. S6A). Then, to quantify the amount of the acquired exosomes, the corresponding standard curve was established (Fig. S6B) by means of commercial immunoassays, that is, Absorbance (A) = 0.126 + 2.08 C_{BSA} (mg/mL), R^2 = 0.995. Overall, TEM, Western blot and bicinchoninic acid (BCA) protein assay results confirmed that exosomes were successfully extracted from the BMMSC supernate for further application.

3.5.2. *Cell viability and drug evaluation biosensing assay*

The cell viability and drug evaluation results from electrochemical biosensing assay were displayed in Fig. 4F. PC12 cells cultured with serum-containing RPMI 1640 medium were set as blank control groups (100% viability). The evident decline in negative control groups indicated serum-free culture impacted neurosecretory capacity seriously. Remarkably, OSI groups demonstrated PC12 cells suffered severe cytotoxicity of H_2O_2. Intervention with nimodipine (5 μM) in 2D and 3D conditions showed discrepancy in biological activity, which was caused by the combined effects of intrinsic drug susceptibility and extracellular matrix. Of note, BMMSC-derived exosomes obviously improved the neurosecretory function across all four PC12 cell lines, since the protective effects of the packaged proteins, RNAs and lipids [43]. Compared with supernatant and drug intervention groups, BMMSC-derived exosomes exhibited superior cytoprotection (Fig. 4F), anti-oxidation effect (Fig. 4G–N), endogenous esterase activity (Fig. S7) and membrane integrity (Fig. S8) both in 2D and 3D conditions, furnishing a promising treatment for OSI. Collectively, the therapeutic and neuroprotective roles of BMMSC-derived exosomes were evident, due to their ability to cross cell membrane barrier and its packaged information on biological function, representing a great potential in mediating neurodegeneration and cytoprotection.

4. Conclusion

In summary, the 3D agarose hydrogel-encapsulated culture mode could greatly mitigate the divergence between the neurosecretion activity and mitochondrial enzyme activity, underscoring the excellent cell functional stability of 3D cultures. The developed electrochemical biosensing assay facilitated rapid, sensitive and *in situ* determination of cell viability within complicated 3D milieu, showing basically alignment with the mitochondrial function assessments whereas not exactly the same. Significantly, we have examined the discrepancy in neurosecretory capacity and drug susceptibility under 2D and 3D culture systems via electrochemical biosensing technique, accompanied by CCK-8. The 3D cell culture was shown to recover natural cell shape, enhance neurotransmitter secretion, and improve stimuli sensitivity to a degree. And the prepared biosensing assay highlighted the remarkable reparative effects of BMMSC-derived exosomes, showing a great potential in neuroprotective treatment. Collectively, the electrochemical biosensing assay can be extended to monitor a variety of cellular processes in intricate 3D surrounding, such as cell differentiation, intervention, senescence and apoptosis.

CRediT authorship contribution statement

Yu Zhong: Writing – original draft, Investigation, Formal analysis, Data curation. **Meng-Meng Liu:** Writing – original draft, Formal analysis. **Xia Cao:** Writing – original draft. **Yun Lei:** Writing – review & editing, Methodology, Formal analysis. **Ai-Lin Liu:** Writing – review & editing, Supervision, Project administration, Funding acquisition, Formal analysis, Conceptualization.

Declaration of competing interest

The authors declare that they have no known competing financial interests or personal relationships that could have appeared to influence the work reported in this paper.

Acknowledgments

The authors gratefully acknowledge the financial support of the National Natural Science Foundation of China (82373838), Joint Funds for the Innovation of Science and Technology, Fujian Province (2020Y9009), the Natural Science Foundation of Fujian Province of China (2023J01551), and Startup Fund for Scientific Research of Fujian Medical University (2023QH2011). The authors would like to thank Yan Hu from the Public Technology Service Center (Fujian Medical University, Fuzhou, China) for technical assistance.

Appendix A. Supplementary data

Supplementary data to this article can be found online at https://doi.org/10.1016/j.talanta.2025.127588.

Data availability

No data was used for the research described in the article.

References

[1] M. Jaganjac, L. Milkovic, N. Zarkovic, K. Zarkovic, Oxidative stress and regeneration, Free Radical Biol. Med. 181 (2022) 154–165.
[2] R. Pardillo-Díaz, P. Pérez-García, C. Castro, P. Nunez-Abades, L. Carrascal, Oxidative stress as a potential mechanism underlying membrane hyperexcitability in neurodegenerative diseases, Antioxidants-basel 11 (2022) 1511.
[3] E.O. Olufunmilayo, M.B. Gerke-Duncan, R.D. Holsinger, Oxidative stress and antioxidants in neurodegenerative disorders, Antioxidants-basel 12 (2023) 517.
[4] Y. Li, K.A. Kilian, Bridging the gap: from 2D cell culture to 3D microengineered extracellular matrices, Adv. Healthcare Mater. 4 (2015) 2780–2796.
[5] A. Hafner, A. Boettiger, The spatial organization of transcriptional control, Nat. Rev. Genet. 24 (2023) 53–68.

[6] S.M. Badr-Eldin, H.M. Aldawsari, S. Kotta, P.K. Deb, K.N. Venugopala, Three-dimensional in vitro cell culture models for efficient drug discovery: progress so far and future prospects, Pharmaceuticals-base 15 (2022) 926.
[7] J. Lou, D.J. Mooney, Chemical strategies to engineer hydrogels for cell culture, Nat. Rev. Chem 6 (2022) 726–744.
[8] J. Kort-Mascort, S. Flores-Torres, O.P. Chavez, J. Jang, L.A. Pardo, S.D. Tran, J. Kinsella, Decellularized ECM hydrogels: prior use considerations, applications, and opportunities in tissue engineering and biofabrication, Biomater. Sci. 11 (2023) 400–431.
[9] M. Zhang, S. Yan, X. Xu, T. Yu, Z. Guo, M. Ma, Y. Zhang, Z. Gu, Y. Feng, C. Du, M. Wan, K. Hu, X. Han, N. Gu, Three-dimensional cell-culture platform based on hydrogel with tunable microenvironmental properties to improve insulin-secreting function of MIN6 cells, Biomaterials 270 (2021) 120687.
[10] R. Orfali, A.Z. Alwatban, R.S. Orfali, L. Lau, N. Chea, A.M. Alotaibi, Y. Nam, M. Zhang, Oxidative stress and ion channels in neurodegenerative diseases, Front. Physiol. 15 (2024) 1320086.
[11] S. Samanta, S. Chakraborty, D. Bagchi, Pathogenesis of neurodegenerative diseases and the protective role of natural bioactive components, J. Am. Nutraceutical Assoc. 43 (2024) 20–32.
[12] A. Ashok, S.S. Andrabi, S. Mansoor, Y. Kuang, B.K. Kwon, V. Labhasetwar, Antioxidant therapy in oxidative stress-induced neurodegenerative diseases: role of nanoparticle-based drug delivery systems in clinical translation, Antioxidants-basel 11 (2022) 408.
[13] Y. Zhang, S. Yu, J.P. Tuazon, J.Y. Lee, S. Corey, L. Kvederis, C. Kingsbury, Y. Kaneko, C.V. Borlongan, Neuroprotective effects of human bone marrow mesenchymal stem cells against cerebral ischemia are mediated in part by an anti-apoptotic mechanism, Neural Regen. Res. 14 (2019) 597.
[14] D. Lo Furno, G. Mannino, R. Giuffrida, Functional role of mesenchymal stem cells in the treatment of chronic neurodegenerative diseases, J. Cell. Physiol. 233 (2018) 3982–3999.
[15] A. Shariati, R. Nemati, Y. Sadeghipour, Y. Yaghoubi, R. Baghbani, K. Javidi, M. Zamani, A. Hassanzadeh, Mesenchymal stromal cells (MSCs) for neurodegenerative disease: a promising frontier, Eur. J. Cell Biol. 99 (2020) 151097.
[16] S. Liu, M. Fan, J.X. Xu, L.J. Yang, C.C. Qi, Q.R. Xia, J.F. Ge, Exosomes derived from bone-marrow mesenchymal stem cells alleviate cognitive decline in AD-like mice by improving BDNF-related neuropathology, J. Neuroinflammation 19 (2022) 35.
[17] S. Samanta, S. Rajasingh, N. Drosos, Z. Zhou, B. Dawn, J. Rajasingh, Exosomes: new molecular targets of diseases, Acta Pharmacol. Sin. 39 (2018) 501–513.
[18] C.N. Ramirez, C. Antczak, H. Djaballah, Cell viability assessment: toward content-rich platforms, Expet Opin. Drug Discov. 5 (2010) 223–233.
[19] M.G. Tian, Y.Y. Ma, W.Y. Lin, Fluorescent probes for the visualization of cell viability, Acc. Chem. Res. 52 (2019) 2147–2157.
[20] Y. Liu, D.A. Peterson, H. Kimura, D. Schubert, Mechanism of cellular 3-(4,5-dimethylthiazol-2-yl)-2,5-diphenyltetrazolium bromide (MTT) reduction, J. Neurochem. 69 (1997) 581–593.
[21] L. Cai, X. Qin, Z. Xu, Y. Song, H. Jiang, Y. Wu, H. Ruan, J. Chen, Comparison of cytotoxicity evaluation of anticancer drugs between real-time cell analysis and CCK-8 method, ACS Omega 4 (2019) 12036–12042.
[22] G.Z. Jiao, X. He, X. Li, J.Q. Qiu, H.Y. Xu, N. Zhang, S.M. Liu, Limitations of MTT and CCK-8 assay for evaluation of graphene cytotoxicity, RSC Adv. 5 (2015) 53240–53244.
[23] Y. Zhong, M.M. Liu, J.C. Li, T.C. Lu, X. Cao, Y.J. Yang, Y. Lei, A.L. Liu, In vitro drug screening models derived from different PC12 cell lines for exploring Parkinson's disease based on electrochemical signals of catecholamine neurotransmitters, Microchim. Acta 191 (2024) 170.
[24] A. Azqueta, H. Stopper, B. Zegura, M. Dusinska, P. Møller, Do cytotoxicity and cell death cause false positive results in the in vitro comet assay? Mutat. Res. Genet. Toxicol. Environ. Mutagen. 881 (2022) 503520.
[25] E. Flampouri, S. Imar, K. Oconnell, B. Singh, Spheroid-3D and monolayer-2D intestinal electrochemical biosensor for toxicity/viability testing: applications in drug screening, food safety, and environmental pollutant analysis, ACS Sens. 4 (2019) 660–669.
[26] M.M. Liu, Z.Z. Guo, H. Liu, S.H. Li, Y. Chen, Y. Zhong, Y. Lei, X.H. Lin, A.L. Liu, Paper-based 3D culture device integrated with electrochemical sensor for the on-line cell viability evaluation of amyloid-beta peptide induced damage in PC12 cells, Biosens. Bioelectron. 144 (2019) 111686.
[27] M.M. Liu, Y. Zhong, Y. Chen, L.N. Wu, W. Chen, X.H. Lin, Y. Lei, A.L. Liu, Electrochemical monitoring the effect of drug intervention on PC12 cell damage model cultured on paper-PLA 3D printed device, Anal. Chim. Acta 1194 (2022) 339409.
[28] B. Li, Y. Li, C. Li, J. Yang, D. Liu, H. Wang, R. Xu, Y. Zhang, Q. Wei, An ultrasensitive split-type electrochemical immunosensor based on controlled-release strategy for detection of CA19-9, Biosens. Bioelectron. 1 (2023) 115180.
[29] B.J. Privett, J.H. Shin, M.H. Schoenfisch, Electrochemical sensors, Anal. Chem. 82 (2010) 4723–4741.
[30] D. Vaudry, P.J.S. Stork, P. Lazarovici, L.E. Eiden, Signaling pathways for PC12 cell differentiation: making the right connections, Science 296 (2002) 1648–1649.
[31] R.H.S. Westerink, A.G. Ewing, The PC12 cell as model for neurosecretion, Acta Physiol. 192 (2008) 273–285.
[32] D. Oprea, C.G. Sanz, M.M. Barsan, T.A. Enache, PC-12 cell line as a neuronal cell model for biosensing applications, Biosensors-basel 12 (2022) 500.
[33] A. Gholizadeh, S. Shahrokhian, A. Iraji zad, S. Mohajerzadeh, M. Vosoughi, S. Darbari, J. Koohsorkhi, M. Mehran, Fabrication of sensitive glutamate biosensor based on vertically aligned CNT nanoelectrode array and investigating the effect of CNTs density on the electrode performance, Anal. Chem. 84 (2012) 5932–5938.
[34] N. Díaz-Prieto, I. Herrera-Peco, A.M.G. de Diego, A. Ruiz-Nuño, S. Gallego-Sandín, M.G.A.G. López, García, M.F. Cano-Abad, Bcl2 mitigates Ca^{2+} entry and mitochondrial Ca^{2+} overload through downregulation of L-type Ca^{2+} channels in PC12 cells, Cell Calcium 44 (2008) 339–352.
[35] K.J. Barnham, C.L. Masters, A.I. Bush, Neurodegenerative diseases and oxidative stress, Nat. Rev. Drug Discov. 3 (2004) 205–214.
[36] Y. Wu, Y. Wang, X. Nabi, Protective effect of Ziziphora clinopodioides flavonoids against H_2O_2-induced oxidative stress in HUVEC cells, Biomed. Pharmacother. 117 (2019) 109156.
[37] H.F. Al-Saedi, Y. Panahi, H.A. Ghanimi, A. Abdolmaleki, A. Asadi, Enhancement of nerve regeneration with nimodipine treatment after sciatic nerve injury, Fund. Clin. Pharmacol. 37 (2023) 107–115.
[38] R.A. Desai, A.L. Davies, N. Del Rossi, M. Tachrount, A. Dyson, B. Gustavson, P. Kaynezhad, L. Mackenzie, M.A. van der Putten, D. Mcelroy, D. Schiza, C. Linington, M. Singer, A.R. Harvey, I. Tachtsidis, X. Golay, K.J. Smith, Nimodipine reduces dysfunction and demyelination in models of multiple sclerosisk, Ann. Neurol. 88 (2020) 123–136.
[39] H.H. Jiang, F.S. Yan, L. Shen, H.F. Ji, Silymarin versus Silibinin: differential antioxidant and neuroprotective effects against H_2O_2-induced oxidative stress in PC12 cells, Nat. Prod. Commun. 11 (2016) 633–636.
[40] W. Tan, Q. Zheng, K. Feng, X. Feng, W. Zhong, C. Liao, S. Li, Y. Liu, W. Hu, Neuroprotection of Gastrodia elata polyphenols against H_2O_2-induced PC12 cell cytotoxicity by reducing oxidative stress, Front. Pharmacol. 13 (2022) 1050775.
[41] F. Zhang, W. Peng, J. Zhang, W. Dong, D. Yuan, Y. Zheng, Z. Wang, New strategy of bone marrow mesenchymal stem cells against oxidative stress injury via Nrf2 pathway: oxidative stress preconditioning, J. Cell. Biochem. 120 (2019) 19902–19914.
[42] C. Liu, T.H. Yang, H.D. Li, G.Z. Li, J. Liang, P. Wang, Exosomes from bone marrow mesenchymal stem cells are a potential treatment for ischemic stroke, Neural Regen. Res. 18 (2023) 2246–2251.
[43] Y. Tang, Y. Zhou, H.J. Li, Advances in mesenchymal stem cell exosomes: a review, Stem Cell Res. Ther. 12 (2021) 1–12.